Forest Discrimination Analysis of Combined Landsat and ALOS-PALSAR Data

E. Lehmann[1], P. Caccetta[1], Z.-S. Zhou[1], A. Mitchell[2], I. Tapley[2], A. Milne[2], A. Held[3], K. Lowell[4], S. McNeill[5]

[1]CSIRO Mathematics, Informatics & Statistics, Floreat, Western Australia – {eric.lehmann, peter.caccetta, zheng-shu.zhou}@csiro.au
[2]Cooperative Research Centre for Spatial Information (CRC-SI), School of Biological, Earth and Environmental Sciences, The University of New South Wales, Sydney, Australia – a.mitchell@unsw.edu.au, hgciant@bigpond.net.au, t.milne@unsw.edu.au
[3]CSIRO AusCover Facility, Canberra, Australia – alex.held@csiro.au
[4]CRC-SI, Department of Geomatics, University of Melbourne, Carlton, Victoria, Australia – klowell@unimelb.edu.au
[5]Landcare Research, Lincoln, New Zealand – mcneills@landcareresearch.co.nz

Abstract – **The joint processing of remote sensing data acquired from sensors operating at different wavelengths has the potential to significantly improve the operation of global forest mapping and monitoring systems. This paper presents an analysis of the forest discrimination properties of Landsat TM and ALOS-PALSAR data when considered as a combined source of information. This study is carried out over a test site in north-eastern Tasmania, Australia. Canonical variate analysis, a directed discriminant technique, is used to investigate the separability of a number of training sites, which are subsequently used to define spectral classes as input to maximum likelihood classification. An accuracy assessment of the classification results is provided on the basis of independent ground validation data, for the Landsat, PALSAR, and combined SAR–optical data. The experimental results demonstrate that: 1) considering the SAR and optical sensors jointly provides a better forest classification than either used independently, 2) the HV polarisation provides most of the forest/non-forest discrimination in the SAR data, and 3) the respective contribution of each of the Landsat and PALSAR bands to the separation of different types of forest and non-forest land covers varies significantly.**

Keywords: land cover, vegetation, mapping, environment, data fusion.

1. INTRODUCTION

The recent deployment of several SAR (synthetic aperture radar) remote-sensing satellites provides a valuable source of Earth observations that complement the currently existing, predominantly optical observations. In parallel, the development of robust methods for large-scale forest monitoring is also becoming increasingly important. These aspects provide a strong motivation for the development of global monitoring systems able to take advantage of the synergies between optical and radar imagery. An important step towards this goal is to address the key aspect of sensor complementarity (adding thematic value by using more than one sensor), and thus to quantify the performance gains achievable by using a SAR–optical data fusion approach.

Several existing studies provide insights into the synergy of optical and SAR data for the mapping of various land covers. Shimabukuro et al. (2007) investigated the relationship existing between Landsat TM and L-band JERS-1 data when considering various land cover types in Amazonia. Their study reported that the SAR data is highly correlated with information derived from Landsat fraction images in the region of interest. The work presented by Erasmi and Twele (2009), which considers Envisat-ASAR and Landsat ETM+ data acquired over a tropical study area in Indonesia, also concluded that the most accurate land cover mapping is achieved by a combination of the optical and SAR sensors. On the other hand, the results provided by Maillard et al. (2008) indicated that the use of C-band Radarsat-1 data did not improve the ASTER-based classification of different types of wetlands and surrounding vegetation in the Brazilian savanna. Another study by Imhoff et al. (1986) found little correlation between L-band SIR-B data and Landsat MSS data for forest canopy characterisation in mangrove jungles of Southern Bangladesh, mostly due to the overriding influence of standing water beneath the forest cover.

This article demonstrates the potential use of combined Landsat TM and ALOS-PALSAR data for forest monitoring, and presents a quantitative analysis and comparison of forest/non-forest (F/NF) discrimination results. It reports some of the findings resulting from the work carried out in the frame of the Forest Carbon Tracking task of the Group on Earth Observations (GEO-FCT, www.geo-fct.org) in a study area in north-eastern Tasmania, Australia. Using a set of training sites, a linear discriminant technique (canonical variate analysis, CVA) is first applied to each data set separately as well as the combined SAR–optical data (created by concatenating the Landsat and PALSAR bands). This supervised approach provides information on the sites' spectral grouping into sub-classes as well as their spectral separation. A variable selection analysis is also performed, producing quantitative metrics on the separation provided by various combinations of the SAR and optical bands. Using the clusters derived in the first step, a maximum likelihood classifier is applied to the individual optical and SAR data as well as the combined data set, resulting in three different classifications. The classification accuracy of each is then summarised against ground validation data.

2. DATA AND STUDY AREA

2.1. Study Area

This work is part of a pilot study carried out for a 66km×50km demonstration area in the Ben Lomond region in north-eastern Tasmania, Australia (Figure 1, left). This area includes one of Australia's national calibration sites defined in the frame of the GEO-FCT initiative. It contains a variety of land covers including rainforests, wet and dry eucalypt forests, non-eucalypt forests, exotic plantations for silviculture, agricultural land, as well as other types of cleared land (deforestation) and urban areas. Significant topographic variations can also be found across the study site, with the terrain elevation varying between 85m and 1510m above sea level.

2.2. ALOS-PALSAR Data

The SAR data over the study area was acquired by the ALOS-PALSAR sensor at L-band (~24cm wavelength) in fine-beam dual-polarisation mode (HH and HV), in an ascending orbit with off-nadir angle of 34.3°. In this study, the SAR data set consists of a mosaic of two PALSAR scenes, namely scene 381/6340 in the west (acquired on October 04, 2008) and scene
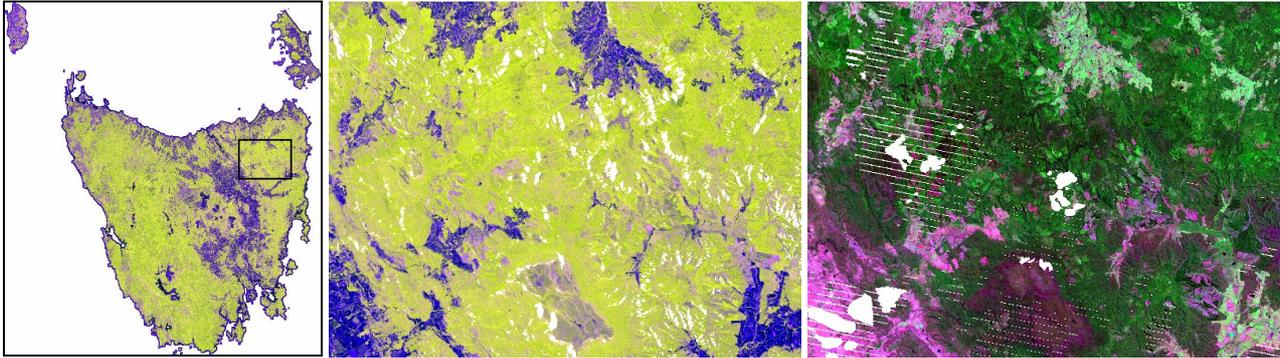
Figure 1. *Left*: SAR mosaic over Tasmania (HH/HV/HH-HV in R/G/B), with box showing the considered 66km×50km study area. *Middle*: ALOS-PALSAR data set (HH/HV/HH-HV in R/G/B) over the study area, with white pixels corresponding to the SAR layover and shadow masks. *Right*: Landsat TM data for the considered area (bands 5/4/2 in R/G/B); white areas indicate regions masked out due to missing data.

380/6340 in the east (acquired on September 19, 2008). The single-look complex data (SLC level 1.1) was pre-processed according to the following steps: 1) 8×2 multi-looking resulting in a 29.8m×25.1m pixel size, 2) speckle filtering by means of adaptive 5×5 Lee filter, 3) radiometric calibration and normalisation, 4) geocoding to 25m pixel size to match the Landsat resolution, using a digital elevation model (DEM) with 25m cell resolution, 5) terrain illumination correction using the 25m DEM, 6) creation of a two-scene mosaic using a gradient mosaicking process, and 7) masking of the data using layover and shadow masks.

This processing sequence provides a mosaic of orthorectified, terrain-corrected and radiometrically calibrated PALSAR scenes at a resolution of 25m (Figure 1, middle). The terrain illumination correction step is necessary to compensate for illumination differences due to the local variations in topography and the side-looking orientation of the SAR sensor. In this work, the terrain correction was carried out using the algorithm described in Zhou *et al.* (2011), which considers the SAR scattering in forested areas together with the local slope angles to derive the terrain correction coefficients.

Texture measures applied to the resulting SAR imagery were not found to add significant value for the F/NF discrimination and classification. This, however, may be due in part to the measures being generated from the pre-processed data, and subsequent work will be carried out to determine whether such measures applied to the raw data are able to improve the results.

2.3. Landsat TM Data

The optical data used in this work was obtained from the existing archive of calibrated Landsat MSS/TM/ETM+ images produced as part of Australia's National Carbon Accounting System (NCAS) (Caccetta *et al.*, 2010). Within this framework, each Landsat scene is processed according to the following steps: 1) orthorectification to a common spatial reference, 2) top-of-atmosphere reflectance calibration, i.e., sun angle and distance correction, 3) correction of scene-to-scene differences using bi-directional reflectance distribution functions, 4) calibration to a common spectral reference using invariant targets, 5) correction for differential terrain illumination, 6) removal of corrupted data such as regions affected by smoke, clouds and sensor deficiencies, and 7) mosaicking of the individual Landsat scenes into 1:1,000,000 map sheets.

Key aspects of these processing steps are discussed in Caccetta *et al.* (2010) and full operational details are given in Furby

(2002). For 2008, the optical data over the study area corresponds to a mosaic of two Landsat scenes (combination of Landsat-5 and Landsat-7 data) acquired on January 14 and February 24, respectively (Figure 1, right).

2.4. Data Coregistration

Ideally, accurate coregistration between the Landsat and SAR images would be established with the use of cross-correlation techniques, image to image registration, and a common elevation model in order to achieve sub-pixel coregistration results. In this work, a common elevation model was used but the PALSAR data was orthorectified using the sensor's orbital parameters while the Landsat data was taken from the legacy NCAS system, which used historic state topographic mapping as its primary control. Spatial cross-correlation of the two data sets was performed using 299 GCPs to check the coregistration of the two data and produced a relative accuracy estimate of 0.6 pixel RMS (at 25m pixel size) with 98% of the residuals below 1.5 pixels, and with no apparent signs of systematic spatial deviations in the displacements between the two images.

The coincidence of acquisition is another important aspect for a joint processing of the data. While not completely true here (Sept./Oct. 2008 vs. Jan./Feb. 2008), the SAR and Landsat data will be assumed to be coincident for the specific purpose of this pilot study. A further discussion of this particular issue is provided in Section 4.

2.5. Reference Data

The selection of training and validation sites used in the analyses was based on a combined consideration of SPOT imagery (2.5m resolution) and a vegetation map product (TASVEG) from the state of Tasmania. The TASVEG map contains information on land cover type, and the SPOT data provides an added check on whether the land cover has deviated or changed from the TASVEG label. In the area of interest, the SPOT image is a mosaic of four scenes acquired between November 2009 and February 2010.

TASVEG is a Tasmania-wide vegetation map produced by the Tasmanian Vegetation Mapping and Monitoring Program within the Department of Primary Industries and Water (www.thelist.tas.gov.au). It comprises 154 distinct vegetation communities mapped at a scale of 1:25,000, and provides a reference that can be used for a broad range of management and reporting applications relating to vegetation in Tasmania. This information is based on a combination of field observations, photo-interpretation and information from other sources such as
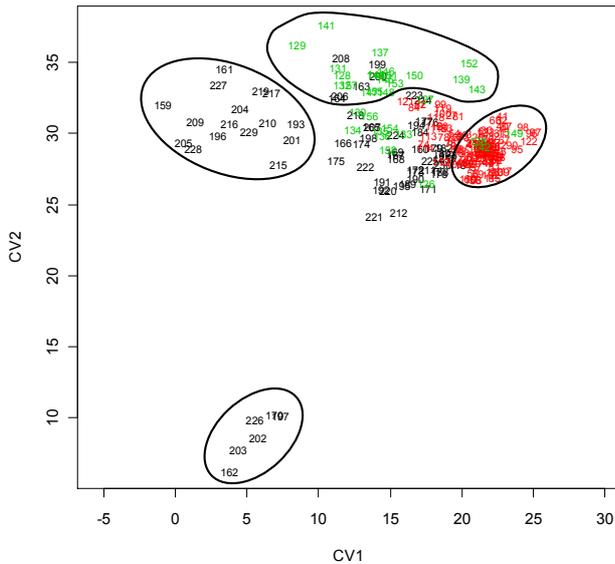
Figure 2. CVA plot for combined SAR–optical data, showing four of the selected six sub-classes (two more classes selected among remaining sites). Sites in red were selected in native forests and mature plantations, sites in black in non-forested areas, and sites in green in harvested/growing plantations.

geological maps and permanent inventory plots. TASVEG is continually revised and updated to reflect changes in the natural environment. In the current area of interest, field work for revision mapping commenced in March 2005 and was completed in October 2008. The selection of training and validation data was also done in conjunction with the Landsat and PALSAR imagery so as to minimise potential errors due to the different acquisition times of the reference data.

3. FOREST/NON-FOREST CLASSIFICATION

The F/NF discrimination analysis carried out in this work was applied to the following three data sets:

1. Landsat only (six spectral bands, thermal band omitted)
2. PALSAR only (two spectral bands)
3. combined SAR and optical data (eight spectral bands), obtained by concatenating the Landsat and PALSAR bands.

Based on the reference data, a total of 230 training sites were selected for the classifications so as to represent a broad range of land cover types over the study area. Each site contains roughly 150 to 200 pixels. The same training sites were used for the analysis of all three data sets, though aggregated separately in each analysis.

3.1. Definition of Spectral Classes using CVA

Using the training data, canonical variate analysis (Campbell and Atchley, 1981) produces a set of orthogonal linear basis functions (canonical vectors, CVs) based on maximising the ratio of between-class separation to within-class variance. The metrics and plots produced by this technique provide the analyst with knowledge from which an informative decision may be made on whether to group, not to group, or reject sites. The analysis also provides information on the reliability with which the selected sub-classes may be mapped. For the three data sets considered in this work, CVA was used to aggregate the training sites into a number of sub-classes to reflect the common spectral characteristics of different land covers. These groupings

included cover types such as water, mature plantations, alpine and subalpine heathland, Buttongrass moorland, etc.

Figure 2 shows an example of CVA plot obtained for the combined PALSAR–Landsat data, with the sites' means displayed in the space defined by the first two CVs. A total of six different sub-classes could be selected for the combined SAR–optical data (four of which are displayed in Figure 2), five for Landsat, and four for PALSAR. The number of sub-classes reflects the ability of each data to discriminate between different land covers. Another measure of separability among the different sites is provided by the canonical roots, which give an indication of the magnitude of the discrimination provided by each canonical vector. The canonical roots resulted as follows:

1. Landsat only: 18.92 8.57 3.24 1.72 1.14 0.53
2. PALSAR only: 24.02 2.94
3. combined: 28.94 12.65 7.69 3.33 1.79 1.31 1.08 0.43

The larger the values of the canonical roots, the greater the separation. These results show that much of the sites' separation using Landsat data is contained in two to three dimensions, and adding the SAR data effectively provides another dimension.

3.2. Maximum Likelihood Classification

The spectral groupings identified in Section 3.1 provided the classes used for a contextual maximum likelihood classifier (MLC), which produces a class label image for each of the three data sets (Kiiveri and Campbell, 1992). Maximum likelihood classification was used due to its ability to provide distance metrics related to the separation of the selected sites and classes. Of interest in this work is the classification accuracy of the F/NF classes. To assess this, the multi-class output of the MLC was collapsed into forest and non-forest labels. Figure 3 shows the resulting F/NF classifications for the PALSAR, Landsat, and combined SAR–optical data over the study area.

A quantitative assessment of these F/NF classification results was carried out on the basis of 88 validation sites, selected independently of the training sites and uniformly distributed over the study area. Table 1 presents the resulting classification accuracy as the percentage of validation sites mapped to the correct forest or non-forest class by the MLC. The middle column (Classification 1) corresponds to the case where the grouping of training sites into sub-classes for the MLC is made independently for each data set, as explained in Section 3.1 (i.e. four sub-classes for PALSAR, five for Landsat, and six for the combined data set). This effectively represents the best classification results achievable for each of the data. These results show that the best classification is achieved when both the SAR and optical data are used jointly, with a 5.7% improvement over the PALSAR-only and 2.3% improvement over Landsat-only classifications.

Table 1. Accuracy of F/NF classifications (percentage of validation sites mapped correctly by the MLC).

	Classification 1	Classification 2
Landsat	92.05 %	89.77 %
PALSAR	88.64 %	87.50 %
combined	94.32 %	94.32 %

The last column in Table 1 corresponds to the results obtained when the six sub-classes of training sites defined for the combined SAR–optical data set are also used in the classification of the PALSAR-only and Landsat-only data. As these six sub-classes correspond to the best number of classes
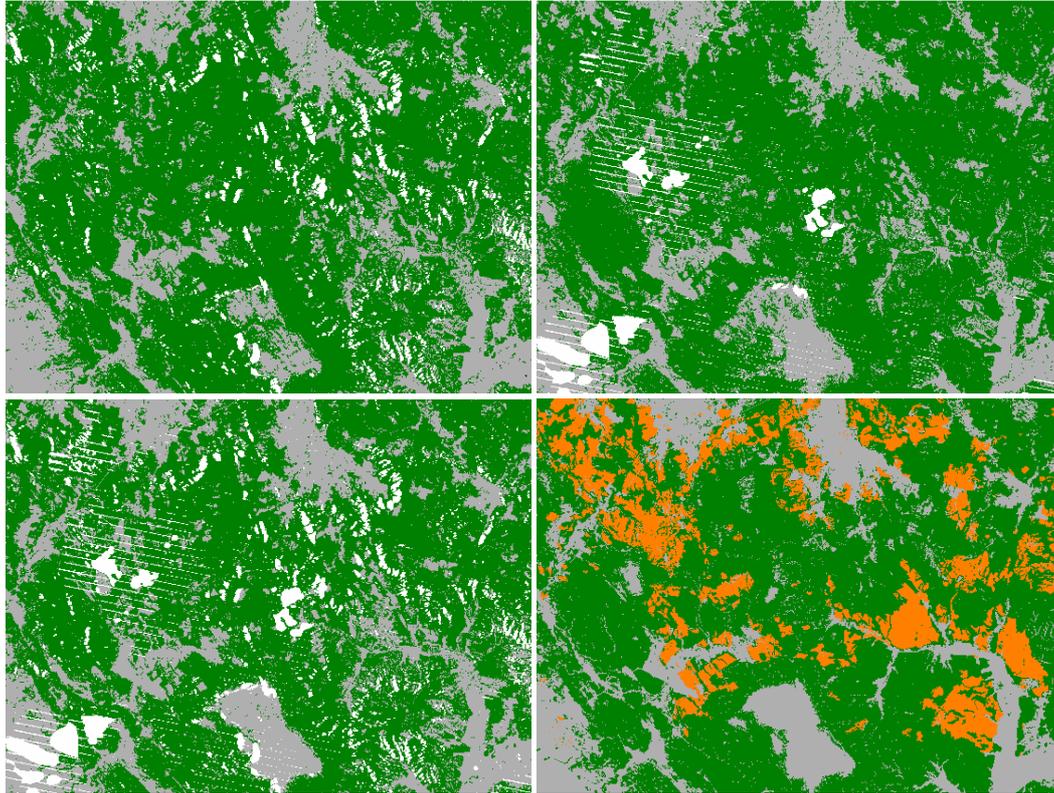
Figure 3. Maximum likelihood F/NF classifications with forest in green and non-forest in grey for PALSAR (*top-left*), Landsat (*top-right*), and combined PALSAR–Landsat data (*bottom-left*). White pixels represent masked areas. *Bottom-right*: TASVEG map with forest in green, non-forest in grey, and plantations (harvested, growing or mature) in orange.

that may be reliably monitored, these results provide an indication of the performance degradation that would result in the joint SAR–optical classifier should one of the input data sets be unavailable (e.g., cloud-affected areas in optical data).

As a typical example of the classification improvements achievable by combining SAR and optical data, Figure 4 focuses on a subset of the MLC outputs in an area known to present difficulties for the classifications. The depicted 20km×15km region is located around Ben Lomond, a large rocky plateau culminating at an altitude of approximately 1300m and covered mostly in highland treeless vegetation (alpine heathland and sedgeland). The bottom-left plot in Figure 4 indicates that the SAR data cannot separate the non-forest area in the middle of the plateau (possibly due to the influence of surface moisture in low stature vegetation at the time of acquisition). On the other hand, the Landsat classification (middle plot, bottom) over-estimates the non-forest areas in the north and west of Ben Lomond. The combination of the PALSAR and Landsat data leads to improved classification results (bottom-right plot) that can be seen to match the TASVEG reference data (top-right plot) much more closely.

3.3. Band Information

Another aspect of interest is to examine the level of information provided by different combinations of Landsat and PALSAR data. To achieve this, a variable selection is performed (MacKay and Campbell, 1982). Table 2 presents the results as the percentage of discrimination provided by various subsets of bands with respect to the information available when all bands are considered simultaneously. This assessment is performed for four scenarios used to check the discrimination existing between different sub-classes of training data (sites from the 'water' sub-class were removed from the analysis due to their clearly-

separable spectral signatures). The column labelled 'F vs. NF' presents generic discrimination results when all the forest sites are compared (contrasted) to all the non-forest sites. This column indicates that: 1) most of the F/NF information provided by the SAR data (68%) is available from the HV polarisation alone (67.8%), 2) the HH polarisation (16.3%) contains less than a quarter of the discrimination information compared to HV (67.8%), and 3) the combination of SAR and optical data significantly improves the forest classification compared to Landsat-only (59.2%) and PALSAR-only (68%).

Table 2. Proportion (in %) of the discrimination information provided by different combinations of the Landsat and PALSAR bands, in comparison to using all available bands.

Bands	F vs. NF	Contrast 1	Contrast 2	Contrast 3
HH	16.3	23.7	31.7	3.9
HV	67.8	50.8	24.0	0.0
HH+HV	68.0	54.7	39.1	4.3
TM (6 bands)	59.2	73.6	41.0	98.6
TM + HH	68.1	82.2	84.5	100.0
TM + HV	99.8	98.9	79.9	98.9
TM+HH+HV	100.0	100.0	100.0	100.0

The last three columns of Table 2 correspond to a contrast of the least separable forest sub-class with each of three neighbouring clusters of non-forest sites (harvested/growing plantations for 'Contrast 1', mixture of alpine heath and Buttongrass moorland for 'Contrast 2', and alpine heathland/sedgeland for 'Contrast 3'), as determined in the CVA for the combined SAR–optical data. These results show that the respective contributions of the SAR and optical data, and that of the HH and HV polarisations, vary significantly when considering the separation of particular sub-classes of forest and non-forest sites.
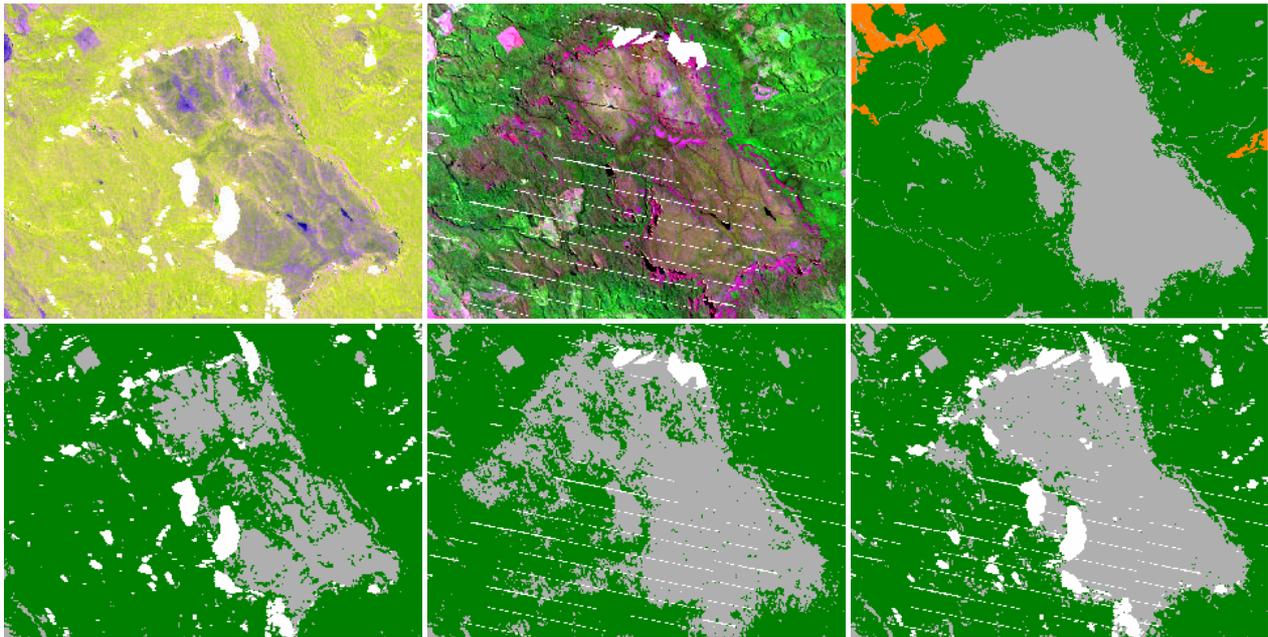
Figure 4. Example of MLC outputs for the Ben Lomond area (20km×15km). In all plots, white pixels indicate masked areas. *Top row, left*: PALSAR data (HH/HV/HH-HV in R/G/B). *Top row, middle*: Landsat data (bands 5/4/2 in R/G/B). *Top row, right*: TASVEG map with forest in green, non-forest in grey, and plantations in orange. *Bottom row, left to right*: maximum likelihood F/NF classifications with forest in green and non-forest in grey for PALSAR, Landsat, and combined PALSAR–Landsat data.

4. CONCLUSION

This paper investigated the forest discrimination properties of a combined SAR and optical data set. Significant classification improvements resulted from the combined data in comparison to using either Landsat or PALSAR separately, despite a significant variation in the respective contributions of the SAR and optical bands to the discrimination of specific land cover types. In accordance with previous literature works, the HV polarisation was here also found to provide most of the discrimination between the forest and non-forest classes compared to HH.

The approach presented in this paper essentially relies on the assumption that the available data are temporally coincident. Should this assumption be invalid, thematic differences between the SAR and optical data resulting from different acquisition dates could be detected in the maximum likelihood classification as a result of the corresponding pixels presenting atypical spectral signatures. A different approach to this issue would be to consider the different data sets as a time series in a multi-temporal classification framework, thus alleviating the need to ensure coincidence. This particular data fusion approach will be the focus of future research.

REFERENCES

Caccetta, P. *et al.*, 2010. Monitoring Australian continental land cover changes using Landsat imagery as a component of assessing the role of vegetation dynamics on terrestrial carbon cycling. In *European Space Agency Living Planet Symposium*. Bergen, Norway.

Campbell, N. and Atchley, W., 1981. The geometry of canonical variate analysis. *Systematic Zoology*, 30(3), pp.268–280.

Erasmi, S. and Twele, A., 2009. Regional land cover mapping in the humid tropics using combined optical and SAR satellite data: a case study from Central Sulawesi, Indonesia. *International Journal of Remote Sensing*, 30(10), pp.2465-2478.

Furby, S., 2002. *Land cover change: specification for remote sensing analysis*, National Carbon Accounting System, technical report no. 9, Australian Greenhouse Office, Canberra.

Imhoff, M. *et al.*, 1986. Forest canopy characterization and vegetation penetration assessment with space-borne radar. *IEEE Transactions on Geoscience and Remote Sensing*, GE-24(4), pp.535-542.

Kiiveri, H. and Campbell, N., 1992. Allocation of remotely sensed data using Markov models for image data and pixel labels. *Australian Journal of Statistics*, 34(3), pp.361-374.

MacKay, R. and Campbell, N., 1982. Variable selection techniques in discriminant analysis – Description. *British Journal of Mathematical and Statistical Psychology*, 35(1), pp.1-29.

Maillard, P., Alencar-Silva, T. and Clausi, D., 2008. An evaluation of Radarsat-1 and ASTER data for mapping veredas (palm swamps). *Sensors*, 8(9), pp.6055-6076.

Shimabukuro, Y. *et al.*, 2007. Quantifying optical and SAR image relationships for tropical landscape features in the Amazônia. *International Journal of Remote Sensing*, 28(17), pp.3831-3840.

Zhou, Z.S. *et al.*, 2011. Terrain slope correction and precise registration of SAR data for forest mapping and monitoring. In *International Symposium for Remote Sensing of the Environment*. Sydney, Australia.